

IMAGES OF AN EQUATORIAL OUTFLOW IN SS433

KATHERINE M. BLUNDELL¹, AMY J. MIODUSZEWSKI², TOM W. B. MUXLOW³,
 PHILIPP PODSIADLOWSKI¹ & MICHAEL P. RUPEN²
Accepted by ApJ Letters

ABSTRACT

We have imaged the X-ray binary SS 433 with unprecedented Fourier-plane coverage at 6 cm using simultaneously the VLBA, MERLIN, and the VLA, and also at 20 cm with the VLBA. At both wavelengths we have securely detected smooth, low-surface brightness emission having the appearance of a ‘ruff’ or collar attached perpendicularly to the well-studied knotty jets in this system, extending over at least a few hundred AU. We interpret this smooth emission as a wind-like outflow from the binary, and discuss its implications for the present evolutionary stage of this system.

Subject headings: Stars: Binaries: Close, Radio Continuum: Stars, Stars: Individual: SS433

1. INTRODUCTION

SS 433 is famous as the first known relativistic jet source in our Galaxy. Red- and blue-shifted optical lines, indicating velocities up to $0.26c$, were discovered by Margon et al. (1979a,b) and interpreted as gas accelerated by oppositely-directed jets (Fabian & Rees 1979; Milgrom 1979). Margon (1984) successfully fit a kinematic precessing jet model, finding an intrinsic jet speed of $\approx 0.26c$, a precession period of 163 days, a cone opening angle of $\sim 20^\circ$, and an inclination to the line-of-sight of $\sim 80^\circ$. This model was spectacularly confirmed by subsequent radio imaging (e.g., Hjellming & Johnston 1981; Vermeulen et al. 1987; Fejes, Schilizzi, & Vermeulen 1988; Vermeulen et al. 1993), which showed precessing twin jets with structure on scales from milli-arcseconds to arcseconds. X-ray emission lines were also discovered which mimic the behavior of the ‘moving’ optical lines (Kotani et al. 1994; Marshall et al. 2001). On the basis of these and other photometric data, SS 433 is believed to be a binary consisting of a compact object [a black hole (Zwitter & Calvani 1989; Fabrika & Bychkova 1990) or a neutron star (Filippenko et al. 1988; D’Odorico et al. 1991)] and an O- or B-type star (Margon 1984). Distance estimates range from 3.1 kpc (Dubner et al. 1998) to 5.5 kpc (Hjellming & Johnston 1981). Here we report the first results from simultaneous radio observations with the Very Long Baseline Array (VLBA), the Multi-Element Radio Linked Interferometer Network (MERLIN), and the Very Large Array (VLA). In addition to the well-known relativistic jets, which will be examined in a series of companion papers, these data reveal smooth radio emission centered on the radio core, extending in a huge ‘ruff’ or collar up to $\gtrsim 40$ milli-arcsec either side of the center.

2. OBSERVATIONS AND IMAGES

We observed SS 433 on 6, 7, and 8 March 1998 for four hours each day with 26 antennas of the VLA; for 10 hrs each day with the 6-antenna MERLIN array; and for 12 hrs each day with the 10-antenna VLBA together with one VLA antenna. The VLA interleaved observations at ~ 20 , 6, and 2 cm; the VLBA, at ~ 20 , 13, and 6 cm; and MER-

LIN observed only at ~ 6 cm. The images shown here were made from the 7 March 1998 data, combining all the arrays at ~ 6 cm, and using the VLBA alone at ~ 20 cm. Images from the independent data taken on 6 and 8 March 1998 confirm all the features reported here.

The 6 cm image shown in Figure 1 was made by combining the 7 March 1998 data from all three arrays. MERLIN observed at 4.993 GHz with a bandwidth of 15 MHz in each of the two independent circular polarizations, using J 1907+0127 as a phase-reference source. The VLBA observed at four independent frequency bands (IF pairs), each 8 MHz wide, in each of the two circular polarizations. Two IF pairs (centered on 4.990 and 4.998 GHz) directly overlap MERLIN’s frequency coverage; the other two are not considered here. J 1907+0127 and J 1929+0507 were used as phase-reference sources, sandwiching 120 s scans on SS 433 between 70 s scans on those two calibrators. The total time on SS 433 (after flagging) at this wavelength was 2.7 hrs. The VLA observed with two IF pairs, each 50 MHz wide, in each of the two circular polarizations, centered on 4985.1 and 4614.9 MHz. The calibrator 1950+081 was used for phase referencing, while occasional observations of 3C 286 set the fundamental flux scale. Initial phase and flux calibration, and fringe-finding for the VLBA, were carried out using standard procedures in NRAO’s Astronomical Imaging Processing System software. The (independently derived) flux scales of the three instruments agreed to better than a few per cent, as determined in overlapping sections of the *uv*-plane. Finally, the MERLIN data, the overlapping IF pairs from the VLBA, and the higher-frequency IF pair from the VLA were concatenated to produce a final, combined data set with full sensitivity on spatial scales ranging from $\sim 10^{-3}$ to ~ 10 arcseconds.

The VLBA observed SS 433 using four IF pairs, each covering 8 MHz in each of the two independent circular polarizations. The central frequencies were 1.404, 1.505, 1.651, and 1.658 GHz, chosen to be spread as far apart as possible within the 18–21 cm band. The same observing scheme was used as at 6 cm. The image shown here however is referenced to J 1928+0507. To avoid uncertainties

¹ University of Oxford, Astrophysics, Keble Road, Oxford, OX1 3RH, U.K.

² National Radio Astronomy Observatory, Socorro, NM 87801, U.S.A.

³ University of Manchester, MERLIN/VLBI National Facility, Jodrell Bank Observatory, Cheshire, SK11 9DL, U.K.

associated with a spatially-variable spectral index, each IF pair was independently imaged (e.g. Fig. 2).

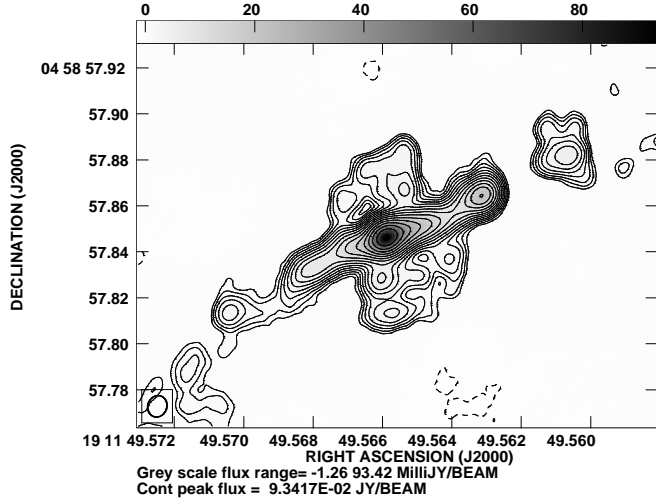


FIG. 1.— 4.99 GHz image of SS 433 on 7 March 1998, combining VLBA, MERLIN, and VLA data. The restoring beam is 9.5×8.2 milliarcseconds (FWHM), oriented at a position angle of $-18^\circ 1$. Contours are $0.5 \times \sqrt{2}^n$ mJy/beam, $n = 1, 2, \dots$

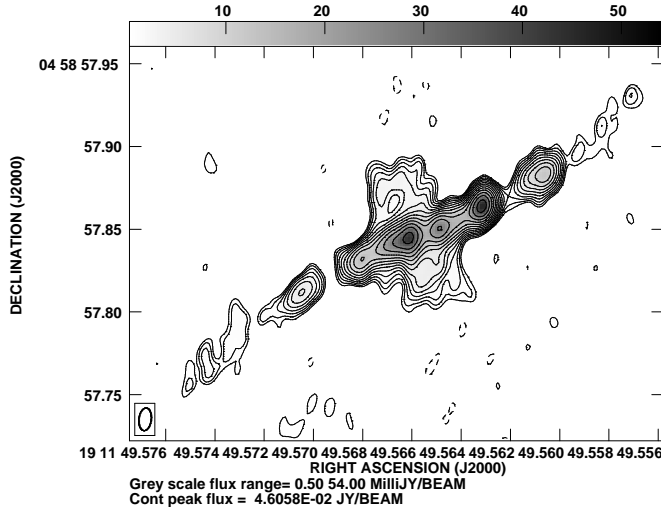


FIG. 2.— 1.6 GHz VLBA image of SS 433 on 7 March 1998. The restoring beam is 13.8×7.5 milliarcseconds (FWHM), oriented at a position angle of $-6^\circ 7$. Contours are $0.5 \times \sqrt{2}^n$ mJy/beam, $n = 1, 2, \dots, 13$.

3. A THERMAL ‘RUFF’ ABOUT THE CENTER OF SS 433

Apart from the well-known knotty jet, the most striking feature of these new images is the smooth emission seen perpendicular to the jet at its center. Since this emission appears to encircle the main jet, we refer to it as a ‘ruff’.

3.1. Is the ‘Ruff’ Real?

Careful testing persuades us that the ‘ruff’ emission is real, and not some calibration or imaging artifact: self-calibration (avoiding the ruff emission itself) and careful data editing cannot remove the emission, which is clearly visible after a single round of phase-only self-calibration based on the brightest portions of the jet. The emission is seen at consistent flux levels, positions, and orientations: in MERLIN and VLBA data reduced independently, and in data from three consecutive days reduced separately.

The ‘ruff’ appears with similar size, brightness asymmetry, position, and flux density (see below), in images made in the individual IF pairs covering 18–21 cm and 6 cm.

3.2. Previous Observations

Paragi and co-workers were the first to report firm evidence for equatorial emission distinct from the jet itself (Paragi et al. 1998, 1999a,b), from VLBA data taken in May 1995. There are some significant differences in what we see, for example they detect equatorial emission which appears to be rather more blobby than smooth; and while our images suggest a ‘halo’ which connects smoothly to (or around) the jet, their naturally-weighted 1.6 GHz image (fig. 1 in Paragi et al. (1999a)) shows a gap of more than 30 mas between the two. It may be that these differences indicate genuine variability in this structure.

Our discovery is the first reported detection of such a smooth feature in SS 433 extended perpendicular to the jets. In part this is because of the high-quality Fourier sampling of these observations, which gives good sensitivity over a wide-range of spatial scales, and also provides much higher fidelity images, less vulnerable to calibration and imaging artefacts.

Evidence of extended emission on much larger angular scales may be seen approximately north and south of the central circular blob in the 330 MHz image of Dubner et al. (1998, figs 1a & 1b).

3.3. Characterizing the ‘Ruff’ Emission

In order to determine the spectral shape of the ‘ruff’ emission we chose *uv*-weighting schemes which gave roughly the same dirty beams for both the 6 and the 18 cm data, CLEANed the images to somewhat below the rms noise levels, and finally convolved the resulting (model+residual) images to a common 10×10 mas Gaussian beam. The resulting total flux densities, measured in identical boxes in all images, which were chosen to avoid the jet but include the full ‘ruff’ emission, are shown in Figure 3a. Note that these are *lower limits* to the total ‘ruff’ emission, since we are excluding any such emission which overlaps with the jet at this spatial resolution. The spectral index for the combined (northern+ southern) emission is $\alpha = -0.12 \pm 0.02$ ($S_\nu \propto \nu^\alpha$, where S_ν is the flux density at frequency ν). This is an interesting result since most resolved synchrotron sources are characterized by $\alpha < -0.4$; indeed, $\alpha = -0.1$ is normally considered the signature of thermal bremsstrahlung emission as is often observed in outflows from symbiotic binaries (Seaquist, Taylor, & Button 1984; Mikolajewska & Ivison 2001). The complication here is that the peak surface brightness corresponds to a brightness temperature of $(2 - 4) \times 10^7$ K at 18 cm, implying a similar *lower limit* to the physical temperature of a thermally-emitting plasma.

The distribution of the flux density perpendicular to the jet is shown in Figure 3b, which suggests that the spectral index is indeed almost flat throughout the ruff, and further shows that the emission extends to $\gtrsim 40$ mas at our sensitivity, or $\sim 120 (d/3 \text{ kpc})$ AU. Note also that the ruff is roughly symmetric about the jet.

3.4. Implications for X-ray emission

If the radio emission is bremsstrahlung from a thermal population of particles then that same population should

co-spatially emit X-rays. The X-ray luminosity is given by $L_x = L_{\text{rad}} \times \exp(-h\nu_x/kT)$ where T is the temperature of the particles (approximated to be the radio brightness temperature), k and h are the Boltzmann and Planck constants, ν_x is the lower frequency of the X-rays whose luminosity L_x is predicted from the radio luminosity L_{rad} . We measure a brightness temperature $T_B \gtrsim 10^7$ K which over-predicts the X-ray luminosity compared with that observed (Margon 1984). Allowing for a significant fraction of the observed X-rays being emitted by the jets means the discrepancy could be as much as an order of magnitude. This could in principle be due to the presence of neutral material in the vicinity of the ruff which would absorb X-rays but not radio emission. Alternatively, it may suggest that the particle population is not Maxwellian.

4. THE ORIGIN OF THE SMOOTH EMISSION

4.1. Theoretical background

The most straightforward interpretation of the radio emission is that it arises from mass outflow from the binary system that is enhanced towards the orbital plane. Such mass loss could either (i) come from the companion (most likely an O or B star), (ii) be a disk wind from the outer parts of the accretion disk or (iii) arise from mass loss from a proto-common envelope surrounding the binary components. The detection of this mass loss may have rather important implications for our understanding of the evolutionary state of this unique system. It has been a long-standing puzzle how SS 433 can survive so long in a phase of extreme mass transfer ($\dot{M} \gtrsim 10^{-5} M_{\odot} \text{ yr}^{-1}$) without entering into a common envelope phase where the compact object spirals completely into the massive companion (for a recent discussion see King, Taam & Begelman 2000). Since the theoretically predicted mass-transfer rate exceeds even the estimated mass-loss rate in the jets ($\dot{M} \sim 10^{-6} M_{\odot} \text{ yr}^{-1}$; Begelman et al. 1980), King et al. (2000) proposed that most of this transferred mass is lost from the system in a radiation-pressure driven wind from the outer parts of the accretion disk (see also King & Begelman 1999). A related problem exists in some intermediate-mass X-ray binaries (IMXBs). Models of the IMXB Cyg X-2 (King & Ritter 1999; Podsiadlowski & Rappaport 2000; Kolb et al. 2000; Tauris, van den Heuvel, & Savonije 2000) show that the system must have passed through a phase where the mass-transfer rate was $\sim 10^{-5} M_{\odot} \text{ yr}^{-1}$, exceeding the Eddington luminosity of the accreting star by many orders of magnitude, without entering into a common-envelope phase, and where almost all the transferred mass must have been lost from the system. The observed emission in SS 433 presented here may provide direct evidence of how such mass loss takes place.

4.2. Evidence for mass out-flows

The existence of a disk-like outflow was first postulated by Zwitter, Calvani, & D'Odorico (1991) to explain the variation with precession phase of the secondary minimum in the photometric light curve. Fabrika (1993) proposed a disk-like expanding envelope caused by mass-loss from the outer Lagrangian point L2 to explain the blue-shifted absorption lines of H I, He I and Fe II (see also Mammano, Ciatti & Vittone (1980), whose spectrum shows that all

the emission lines seen in SS 433 have P-Cygni profiles indicating the presence of outflowing gas). Filippenko et al. (1988) observe a remarkable double peaked structure for the Paschen lines, with speeds close to 300 km s^{-1} .

4.3. Estimates of \dot{M} and the windspeed

If we assume that the observed radio emission is due to bremsstrahlung, we can obtain a rough estimate for the mass-loss rate, \dot{M} , in this equatorial outflow. For this purpose, we assume that the outflow is radial but confined to an angle α with respect to the orbital plane of the binary. For a simple wind mass-loss law, the mass density, ρ , of the outflow then depends on the distance r from the system according to $\rho = \dot{M}/(4\pi \sin \alpha r^2 v_{\infty})$, where v_{∞} is the outflow velocity at infinity. At a particular radio frequency ν , the outflow will be optically thick to some distance \bar{r}_{ν} .

Assuming that we see all the radio emission from the optically thin part of the outflow and are observing the system close to the orbital plane (both assumptions are only approximately true and ignore geometrical complications), a rough estimate for the mass-outflow rate is

$$\dot{M} \simeq 1.6 \times 10^{-4} M_{\odot} \text{ yr}^{-1} \quad (1)$$

$$\times S_{50}^{3/4} d_3^{3/2} v_{300} \nu_{1.4}^{-1/2} \bar{g}_{10}^{-1/2} (\sin \alpha)_{30}^{1/4},$$

where $S_{50} = S_{\nu}/50 \text{ mJy}$, $d_3 = d/3 \text{ kpc}$, $v_{300} = v_{\infty}/300 \text{ km s}^{-1}$, $\nu_{1.4} = \nu/1.4 \text{ GHz}$, $\bar{g}_{10} = \bar{g}/10$ (\bar{g} is the Gaunt factor for free-free emission; see e.g., Rybicki & Lightman 1979), $(\sin \alpha)_{30} = \sin \alpha / \sin 30^\circ$.

One of the major uncertainties in this estimate is the velocity of the outflow, though a velocity of $\sim 300 \text{ km s}^{-1}$ is similar to that of the lines by Filippenko et al. (1988) and is close to the characteristic orbital velocity of SS 433, as one might expect for an outflow from the binary system rather than either binary component. Furthermore, if this outflow started soon after the supernova explosion which formed the compact object $\sim 10^4$ yr ago and whose impressively circular remnant is seen clearly in the images of Dubner et al. (1988), a velocity of $\sim 300 \text{ km s}^{-1}$ implies an extent of the outflow of $\sim 3 \text{ arcmin}$ (for $d = 3 \text{ kpc}$). Indeed, this is exactly the size of the extended smooth emission seen by Dubner et al. (1998) and suggests that this may be the outer extent of the same outflow.

The above estimate for \dot{M} would imply that the outflow is optically thick at a frequency of $\sim 1 \text{ GHz}$ to a distance of $r \sim 10^{15} \text{ cm}$ and that the radio emission from the central region of the jet would be somewhat attenuated (although this will also depend on the exact geometry of the outflow and its orientation to the line of sight).

It also suggests that the outflow is moderately optically thick in the optical and that part of the observed visual extinction to the system ($A_V = 7.8$, Margon 1984) may be due to the outflow, as postulated by Zwitter et al. (1991).

The inferred mass-loss rate, $\dot{M} \sim 10^{-4} M_{\odot} \text{ yr}^{-1}$, is much higher than any reasonable mass-loss rate from an O-star primary and suggests that it is connected with the unusual short-lived phase SS 433 is experiencing (see § 4.1). It could be mass loss from a common envelope that has already started to form around the binary, or a hot coronal wind from the outer parts of the accretion disk driven, e.g., by the X-ray irradiation from the central compact source.

5. SUMMARY

With unique sampling in the UV-plane, we have imaged the SS 433 system at 6 cm and 20 cm and securely detected at both wavelengths smooth emission extending over a few hundred AU perpendicular to the jet axis. The most likely interpretation of this radiation is emission from matter which has been ejected from the disk as a thermal

wind with an outward speed of $\sim 300 \text{ km s}^{-1}$.

K.M.B. thanks the Royal Society for a University Research Fellowship. MERLIN is a U.K. national facility operated by the University of Manchester on behalf of PPARC. The VLBA and VLA are facilities of NRAO operated by AUI, under cooperative agreement with the NSF.

REFERENCES

D'Odorico, S., Osterloo, T., Zwitter, T., & Calvani, M., 1991, *Nature*, 353, 329
 Dubner, G. M., Holdaway, M., Goss, W. M., & Mirabel, I. F., 1998, *AJ*, 116, 1842
 Fabian, A. C. & Rees, M. J., 1979, *MNRAS*, 187, 13P
 Fabrika, S. N. & Bychkova, L. V., 1990, *A&A*, 240, L5
 Fabrika, S. N., 1993, *MNRAS*, 261, 241
 Fejes, I., Schilizzi, R. T., & Vermeulen, R. C. 1988, *A&A*, 189, 124
 Filippenko, A. V., Romani, R. W., Sargent, W. L. W., & Blandford, R. D., 1988, *AJ*, 96, 242
 Hjellming, R. M. & Johnston, K. J. 1981, *Nature*, 290, 100
 King, A. R., Taam, R. E., & Begelman, M. C. 2000, *ApJ*, 530, L25
 King, A. R. & Begelman, M. C. 1999, *ApJ*, 519, L169
 King, A. R. & Ritter, H. 1999, *MNRAS*, 309, 253
 Kotani, T., et al., 1994, *PASJ*, 46, L147
 Kolb, U., Davies, M, King, A., & Ritter, H. 2000, *MNRAS*, 317, 438
 Mammomo, A., Ciatti, F., & Vittone, A. 1980, *A&A*, 85, 14
 Margon, B. 1984, *ARA&A*, 22, 507
 Margon, B., et al. 1979a, *ApJ*, 230, L41
 Margon, B., Ford, H. C., Grandi, S. A., & Stone, R. P. S., 1979b, *ApJ*, 233, L63
 Marshall, H., Canizares, C. R. & Schulz, N. S., 2001, in press at *ApJ*
 Milgrom, M., 1979, *A&A*, 76, L3
 Mikolajewska, J. & Ivison R. J., 2001, *MNRAS*, 324, 1023
 Paragi, Z., Vermeulen, R. C., Fejes, I., Schilizzi, R. T., Spencer, R. E., & Stirling, A. M. 1998, *New A. Rev.*, 42, 641
 —, 1999a, *A&A*, 348, 910
 —, 1999b, *New A. Rev.*, 43, 553
 Podsiadlowski, Ph. & Rappaport, S. 2000, *ApJ*, 529, 946
 Rybicki, G. B. & Lightman, A. P. 1979, John Wiley & Sons
 Seaquist, E. R., Taylor, A. R., & Button, S. 1984, *ApJ*, 284, 202
 Tauris, T. M., van den Heuvel, E. P. J., & Savonije, G. J. 2000, *ApJ*, 530, L93
 Vermeulen, R. C., Schilizzi, R. T., Icke, V., Fejes, I., & Spencer, R. E., 1987, *Nature*, 328, 309
 Vermeulen, R. C., Schilizzi, R. T., Spencer, R. E., Romney, J. D., & Fejes, I., 1993, *A&A*, 270, 177
 Zwitter, T. & Calvani, M., 1989, *MNRAS*, 236, 581
 Zwitter, T., Calvani, M., & D'Odorico, S. 1991, *A&A*, 251 92

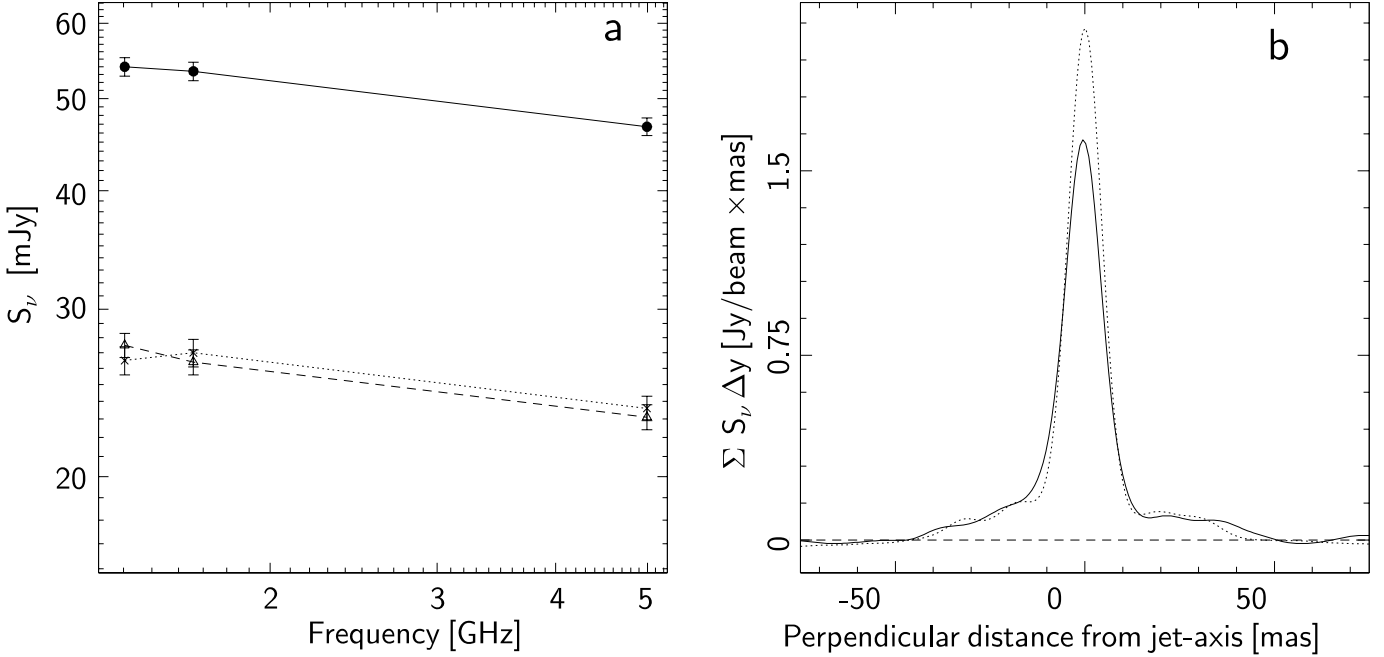


FIG. 3.— *a*: The total flux density in the ‘ruff’ emission as a function of frequency (see text). Crosses: northern emission; triangles: southern emission; filled circles: sum of northern and southern emission. *b*: The flux density integrated over 40 mas strips parallel to the jet, as a function of distance perpendicular to the jet, at 10 mas resolution. The solid line is 18 cm, the dotted line the 6 cm data. Note the flat spectrum of the ‘ruff’ emission, compared to the inverted spectrum of the (self-absorbed) jet core.